ELSEVIER

Thin Solid Films 253 (1994) 247–253

thin solid films

Atmosphere influence on in-situ ion beam analysis of thin film growth

Yuping Lin[a,b], Alan R. Krauss[a], Robert P. H. Chang[b], Orlando H. Auciello[c], Dieter M. Gruen[a], J. Albert Schultz[d]

[a]*Materials Science and Chemistry Divisions, Argonne National Laboratory, Argonne, IL 60439, USA*
[b]*Department of Materials Science and Engineering, Northwestern University, Evanston, IL 60208, USA*
[c]*Microelectronics Center of North Carolina, Research Triangle Park, NC 27709, USA*
[d]*Ionwerks Inc., Houston, TX 71310, USA*

Abstract

In-situ non-destructive surface characterization of thin film growth processes in an environment of chemically active gas at pressures of several millitorrs is required both for the understanding of growth processes in multicomponent films and layered heterostructures and for the improvement of process reproducibility and device reliability. We have developed a differentially pumped pulsed ion beam surface analysis system that includes ion scattering spectroscopy (ISS) and direct recoil spectroscopy (DRS), coupled to an automated ion beam sputter deposition system, to study film growth processes in an environment of chemically active gas, such as required for the growth of oxide, nitride or diamond thin films. The influence of gas-phase scattering and gas–surface interactions on the ISS and DRS signal intensity and peak shape has been studied. From the intensity variation as a function of ambient gas pressure, we have calculated the mean free path and the scattering cross-section for several combinations of primary ion species and ambient gas. Depending on the system geometry and the combination of primary beam and background gas, it is shown that surface-specific data can be obtained during thin film growth at pressures ranging up to several millitorrs. Detailed information such as surface composition, structure and film growth mechanism may be obtained in real time, making ion beam analysis an ideal non-destructive in-situ probe of thin film growth processes.

Keywords: Ion scattering; Sputtering; Surface composition; Surface structure

1. Introduction

Increased structural complexity and stringent constraints on composition and layer thicknesses in electronic devices are providing a strong incentive for the development of non-intrusive diagnostic techniques that can be used in the thin film growth environment as a means of in-situ characterization of growth processes. Since film growth typically happens on the uppermost one to two atomic layers, and extremely sharp interfaces are important to many multilayer structures, it is desirable to utilize an analytical method which has a surface specificity of one to two atomic layers. However, most such surface-analytical methods involve instrumentation that physically obstructs access to the substrate and are therefore incompatible with simultaneous film deposition. In addition, the fabrication of multicomponent oxide films, such as high temperature superconductors and ferroelectric materials, is usually carried out in an atmosphere consisting of oxygen at a partial pressure of several millitorrs, whereas most surface-analytical instruments require ultrahigh vacuum conditions. Optical probes such as spectroellipsometry do not obstruct line of sight to the substrate and are capable of operation in an ambient gas, but they provide information that is integrated over the penetration depth of light in the sample and are therefore not monolayer surface specific [1].

Time-of-flight ion scattering spectroscopy (ISS) and direct recoil spectroscopy (DRS) [2, 3] have been traditionally applied to determination of surface structure and composition under ultrahigh vacuum conditions. However, Schmidt et al. [4] demonstrated that, by differentially pumping the detector and ion beam line, it is possible to perform DRS with the sample immersed in gas at ambient pressures as high as 1 Torr. DRS is very sensitive to light elements, but it is more difficult to obtain detailed structural information that may be extracted from ISS data. The two methods have common hardware and software requirements and therefore form a powerful combination when deployed in a single instrument.

Elsevier Science S.A.
SSDI 0040-6090(94)04652-M

We have developed [5] an ISS–DRS spectrometer with differentially pumped ion source and detectors for the in-situ study of thin film deposition, as well as surface adsorption and oxidation, in relatively high (millitorr range) background gas pressure environments. The volume of the high pressure region is much larger than in the original design of Schmidt et al., resulting in simplified beam alignment and the ability to install thin film deposition apparatus at the expense of a lower maximum background pressure. The differential pumping concept is also applicable to a third form of ion beam surface-analytical spectroscopy, namely mass spectroscopy of recoiled ions (MSRI) [4].

Au, Pb and Cu films were deposited on an Si(100) substrate and analyzed in the presence of various background gases to verify the utility of pulsed ion beam surface anlaysis methods for in-situ characterization of thin film deposition processes. It is anticipated that, in addition to gas-phase scattering, the spectra for the Cu and Pb samples will be affected by oxygen adsorption. The study of growth processes involving coadsorption of two, three or more elements, as well as composition and structure changes due to ambient atmosphere and heat treatment are of great interest in surface science and semiconductor device technology [6–8].

2. Theory

In order to explore the high pressure limit of our system, the influence of gas-phase scattering on the intensity of ISS and DRS beams was studied. According to the gas-phase kinetic theory, the relationship between the scattered–recoiled signal intensity I and the mean free path λ of the beam in an ambient gas is

$$I = I_0 c \exp\left(-\frac{d}{\lambda}\right) \quad (1)$$

where I_0 is the primary beam intensity, c is a constant that includes the surface particle reflection coefficient and detector collection efficiency, and d is the total distance that the beam travels through the ambient gas region, while $\lambda = kT/p\sigma$, k is Boltzmann's constant, T is the gas temperature, p is the pressure and σ is the scattering cross-section. Therefore

$$\ln(I) = \ln(I_0 c) - \frac{dp\sigma}{kT} \quad (2)$$

The value of σ depends on the primary ion species, the ambient gas and the kinetic energy of primary ions. Measurements are presented in Section 4 for 10 keV primary-beam ISS and DRS signal attenuation.

3. Instrumentation

The experimental apparatus is shown schematically in Fig. 1. It consists of an ultrahigh vacuum surface analysis chamber with ISS–DRS, coupled to a multi-target ion beam sputter deposition system through a 6 mm aperture for sputtered flux confinement and differential pumping as described elsewhere [9]. The base pressure of the analysis chamber is about 5×10^{-10} Torr when pumped by ion and Ti sublimation pumps. During deposition the gas load is too high for the ion pump, and a 250 l s^{-1} turbomolecular pump connected via a 10 cm gate valve provides pumping with a base pressure of approximately 2×10^{-8} Torr. Two 60 l s^{-1} turbomolecular pumps are also attached to the fittings in which the electron multiplier detectors are mounted. Helium, neon and oxygen were introduced into the chamber through a leak valve, while argon was introduced via the capillaritron ion source [10] in the sputtering chamber. The ISS–DRS instrumentation and sputter deposition system [11, 12] have been described in detail in previous publications. Two quartz crystal monitors QC1 and QC2 in Fig. 1 are located in the sputtering and analysis chambers respectively. QC1 provides a continuous readout during deposition, and QC2 was installed at the substrate position for purposes of calibration of the flux incident upon the substrate. A more accurate calibration as a function of background gas species and pressure will be made by directly measuring the deposited film thickness using an atomic force microscope. The inert-gas ion beam (normally set at 10 keV) is produced by an Atomika W610 telefocus ion source.

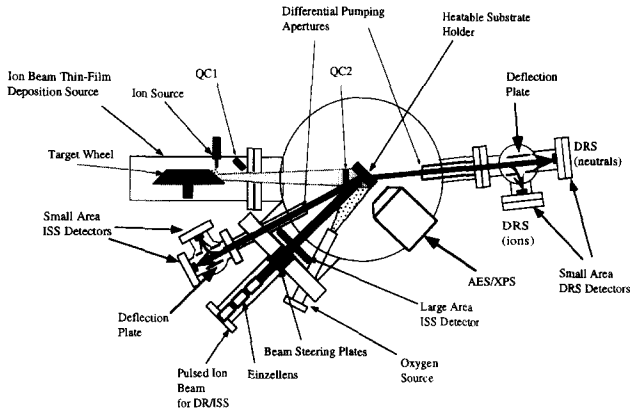


Fig. 1. Differentially pumped ISS–DRS and ion beam thin film deposition system: AES/XPS, Auger electron spectroscopy–X-ray photoelectron spectroscopy.

For ISS the pulsed ion beam is incident on the sample that is located on the chamber axis and is scattered at an angle of 165° into a channel electron multiplier detector. To protect the detector from damage during ISS analysis at elevated pressure, a 1.5 mm differential pumping aperture is located between the detector housing and analysis chamber to keep the detector below the 10^{-5} Torr maximum operating pressure. A second differentially pumped detector is positioned in the forward direction at a scattering angle of

25° to detect direct recoil-ejected surface atoms for light elements (H, C and O). The total distance traversed by the incident primary and scattered–recoiled signal atom in the present system is 0.6 m, distributed as 0.45 m for the incident beam and 0.15 m for the exit beams. With the addition of another pumping stage at the end of the beam line and repositioning of the detector apertures, this will be reduced to approximately 0.3 m without loss of signal.

4. Results and discussion

Au foil was chosen to study the ISS signal attenuation as a function of ambient pressure, because Au does not react with ambient gases at room temperature and has a well-defined reproducible peak shape for all ion beam species used in the present experiment. The foil was cleaned by bombarding with a continuous 0.1 μA 10 keV Ar^+ beam, with intermittent monitoring via pulsed-beam ISS–DRS until a well-defined Au peak was obtained, with a sharp rise on the low time-of-flight side and little or no short time-of-flight "tailing" that would be indicative of a light-atom (H, C and O) contamination layer. The analysis chamber was then backfilled to various pressures of He, Ne, Ar and O_2, and the ISS data were obtained using 10 keV He^+, Ne^+ and Ar^+ primary ion beams. Each spectrum required a data acquisition time of approximately 2 min, utilizing a beam current of ~0.5 nA, rastered into an area of 1 mm^2. The resulting beam dose was about 10^{13} ions cm^{-2} per spectrum, which was sufficiently low to cause negligible damage during the data acquisition period.

Data for 10 keV Ar^+ incident on the Au sample in an oxygen background are shown in Fig. 2 for ambient pressures of 6.8×10^{-8} Torr (curve (a)), 1.0×10^{-4} Torr (curve (b)), 5.0×10^{-4} Torr (curve (c)) and 1.0×10^{-3} Torr (curve (d)). The spectra are all characterized by a relatively sharp onset on the high velocity side of the peak and a long tail on the low velocity side, resulting from multiple scattering from subsurface gold atoms in the polycrystalline foil. The intensity decreases as the gas pressure increases, but the shape of the peak and position of the high velocity edge do not change. Therefore the reduction in ISS intensity is believed to be caused primarily by gas-phase scattering of the primary ion beam and scattered beam.

The intensity of the ISS Au peak is plotted in Figs. 3(a), 3(b), 3(c) and 3(d) for He^+, Ne^+ and Ar^+ primary ion beams incident on a gold foil immersed in atmospheres of He, Ne, Ar and O_2 respectively as a function of *pd*, the product of the pressure of the background gas and the distance traveled through the gas. The maximum pressure measured was limited in some cases by the fact that the pressure at the detector exceeded the safe operating limit of the electron multiplier. This limit will be increased in the future by modifying the size and position of the detector aperture in such a way as to obtain better pumping along with increased signal intensity.

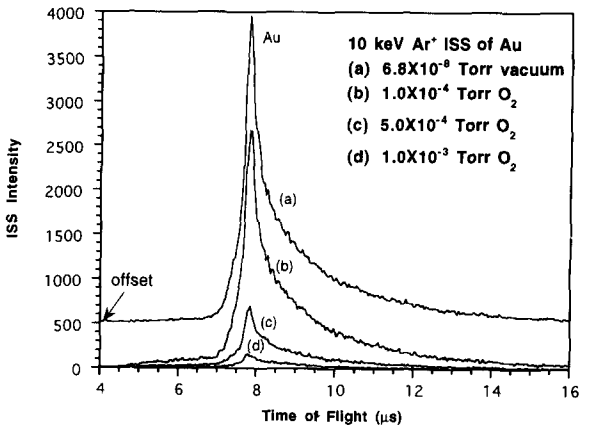


Fig. 2. Ion scattering spectra for a 10 keV Ne^+ beam incident on sputter-cleaned Au foil in different oxygen pressures.

When plotted on a semi logarithmic scale, the data fall on a straight line in agreement with Eq. (2), allowing the cross-section and mean free path to be determined from the slope of the straight line. The experimentally determined values of σ for the 10 keV ions shown in Table 1 vary from 0.50 to 3.57 $Å^2$, with the smallest values for the He atmosphere and the largest values for Ar. It should be noted that the values listed in Table 1 are averages weighted in the ratio of the inbound and outbound path lengths, i.e. 75% for the incident ion beam and 25% for the outgoing beam (primarily neutrals). Generally the cross-section is larger for ion–molecule collisions than for neutral atom–molecule collisions, and the cross-section decreases as the kinetic

Table 1
The experimentally determined cross-section σ and mean free path values λ, determined from the data in Fig. 3 for various gases exposed to 10 keV He^+, Ne^+ and Ar^+ beams

Primary ion	Gas	σ (m^2)	λ ($N\,m^{-1}$)
He^+	He	3.7×10^{-20}	0.113
Ne^+	He	2.5×10^{-20}	0.163
Ar^+	He	3.9×10^{-20}	0.105
He^+	Ne	4.4×10^{-20}	0.094
Ne^+	Ne	7.8×10^{-20}	0.053
Ar^+	Ne	5.7×10^{-20}	0.073
He^+	Ar	1.3×10^{-19}	0.033
Ne^+	Ar	5.8×10^{-20}	0.072
Ar^+	Ar	1.8×10^{-19}	0.023
He^+	O_2	1.5×10^{-19}	0.028
Ne^+	O_2	1.1×10^{-19}	0.038
Ar^+	O_2	1.7×10^{-19}	0.025

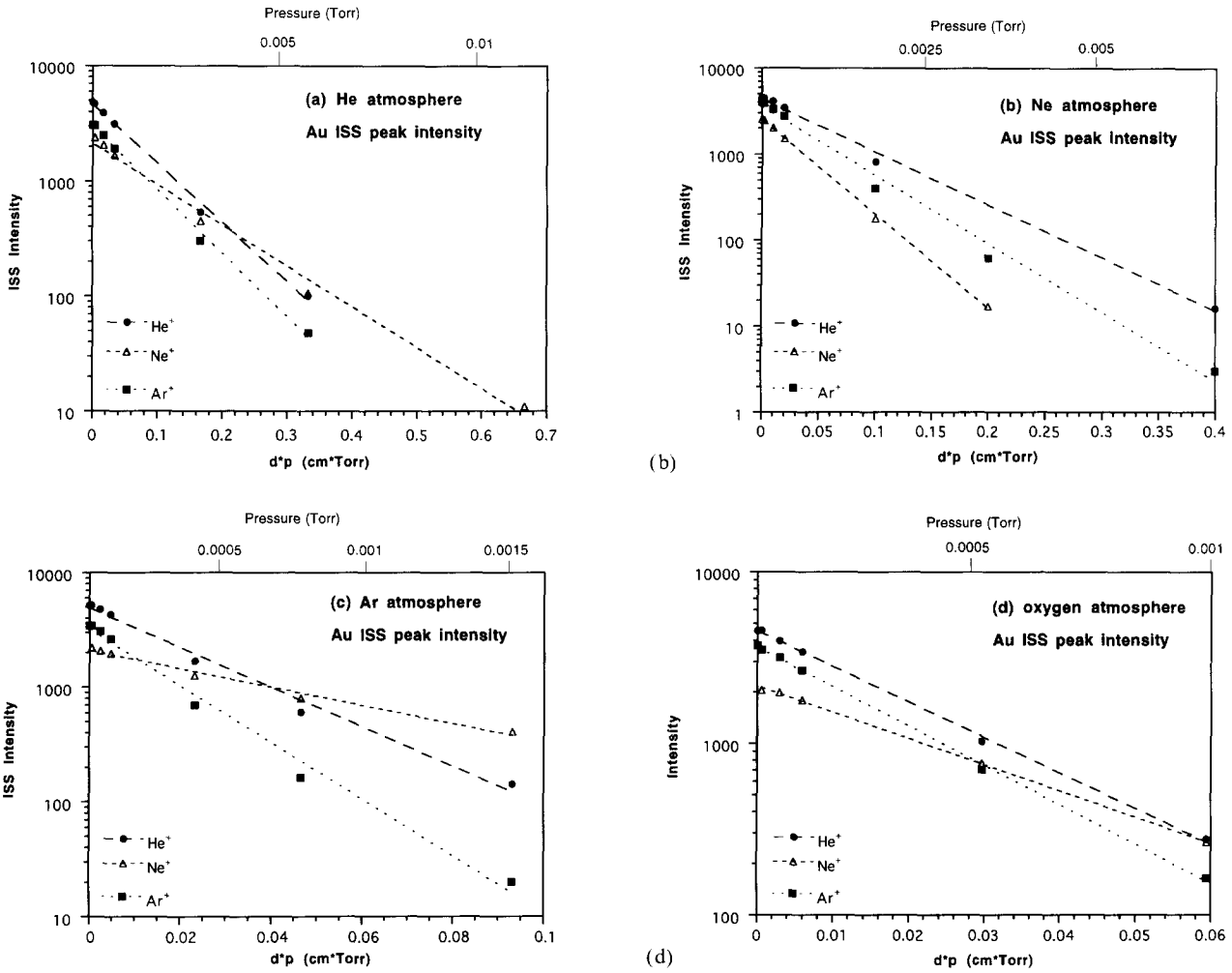


Fig. 3. The intensity of the ISS Au peak for He^+, Ne^+ and Ar^+ primary ion beams incident on a gold foil immersed in atmospheres of (a) He, (b) Ne, (c) Ar and (d) O_2 as a function of *pd*, the product of the pressure of the background gas and the distance traveled through the gas.

energy of the primary ions increases [13]. However, since the Au target atom is much heavier than the primary ions, there is little difference between the velocities of the incident and scattered primary ions, and the values listed in Table 1 may be considered representative of the 10 keV primary-ion beam. The resulting cross-section value for Ar^+–Ar is consistent with reported values for ion–neutral atom collisions [13].

Fig. 4 shows direct recoil spectra for a 10 keV Ar^+ beam incident on sputter-cleaned Au foil as a function of neon backfill pressure. Before admitting Ne, some H, C, O, S and Ru were seen in addition to Au. H, C, O and S are surface contaminants, which show the ultra-high sensitivity of DRS to surface light elements. Ru represents a "memory effect" resulting from recent Ru sputtering experiments in the sample chamber. When the Ne is first introduced, there are slight increases in the H and C signals, together with a decrease in the intensity of the Au signal. This is thought to be due to the admission of a slight amount of hydrocarbon impurity from the Ne gas admission line. As the Ne pressure

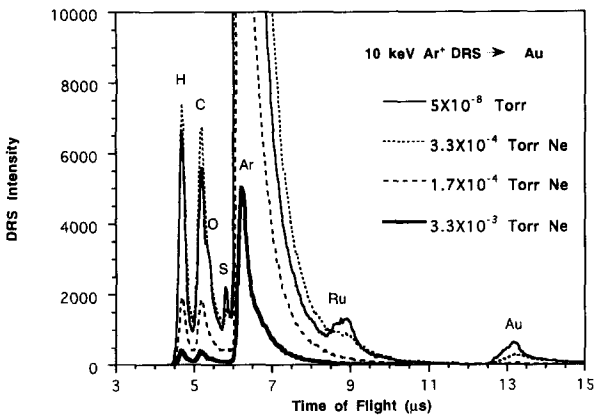


Fig. 4. Direct recoil spectra for a 10 keV Ar^+ beam incident on sputter-cleaned Au foil in different Ne backfill pressures.

is raised further, all signal intensities decrease as a result of gas-phase scattering as shown in Fig. 5. The decrease in signal intensity is comparable with that experienced for ISS. However, the Au direct recoil atoms are much slower than the primary ions, and the collision

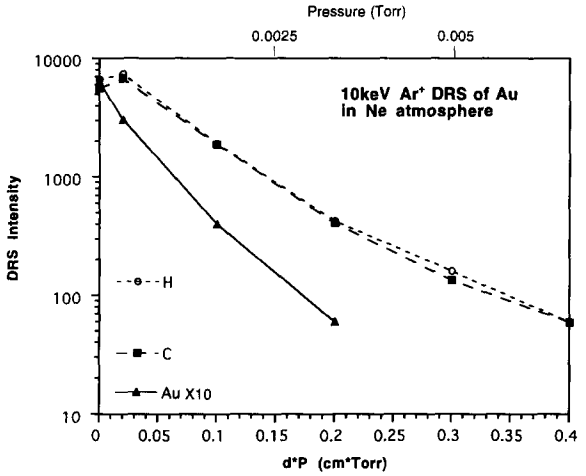


Fig. 5. The DRS intensities of H, C and Au peaks for Ne^+ primary ion beams incident on a gold foil immersed in Ne atmosphere as a function of *pd*.

cross-section for the inbound primary ion and outbound direct recoil atom may be significantly different. A more detailed comparison of ISS, DRS and MSRI signal intensities in ambient gases is in preparation.

A gold film ~9.5 Å thick was deposited on the Si substrate at room temperature using a capillaritron ion source producing 2–3 mA of 4 keV Kr^+ to sputter an Au target. Owing to the gas flow from the capillaritron ion source, the sputtering chamber pressure was 6×10^{-4} Torr and the analysis chamber pressure was 5×10^{-4} Torr. The deposition rate measured by the quartz crystal monitor in the sputtering chamber was 0.85 Å s^{-1}, corresponding to ~0.1 Å min^{-1} at the Si(100) substrate mounted on the sample holder on the axis of analysis chamber. The low deposition rate on the substrate was caused by the long distance between the substrate and the target (0.4 m). However, the achieved deposition rate is adequate for real-time nucleation and initial growth studies. The primary ions were 10 keV Ne^+ with a pulse width of 100 ns. The time-averaged beam current was about 0.5 nA with a spot size of ~1 mm^2. Each spectrum presented was acquired in about 1 min of beam-on time, corresponding to a dose of $\sim 5 \times 10^{12}$ ions cm^{-2}. At this dose, less than 1% of the surface atoms are sputtered. Similarly, we have found that ~1% of the atoms within the collision cascade volume are displaced from their lattice sites. A number of comparisons of surface contamination rate and erosion of ultrathin deposits in bombarded and non-bombarded areas confirm that time-of-flight ISS–DRS can be regarded as non-destructive methods for in-situ characterization of thin-film growth processes.

Fig. 6 shows the ion scattering spectra taken with a 10 keV Ne^+ beam during Au deposition on Si(100). Starting at the bottom of the figure, each spectrum was taken after deposition for an additional 5 min, corresponding to a growth of ~0.5 Å per spectrum. Initially,

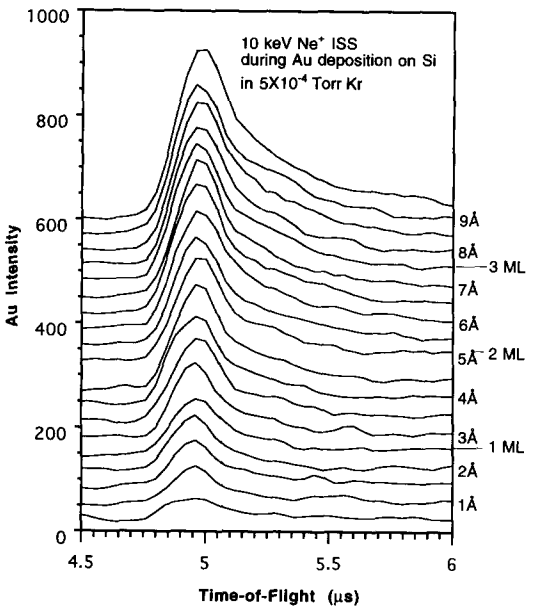


Fig. 6. 10 keV Ne^+ ion scattering spectra during Au deposition in Kr at 5×10^{-4} Torr.

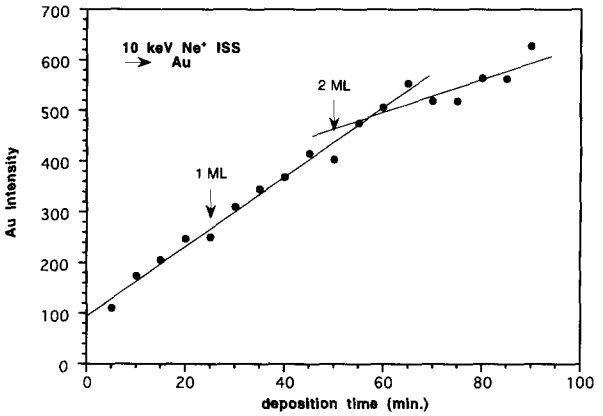


Fig. 7. Au ISS peak intensity during deposition as a function of the deposition time.

the Au peak is reasonably symmetric, corresponding to a single atomic layer and indicating that the first monolayer of Au is deposited in a layer-by-layer growth mode. However, starting at about 2.5 Å (about 1 monolayer (1 ML)), a long time-of-flight tail begins to form, becoming more prominent as the film thickness exceeds 5.0 Å (~2 ML) and growing in intensity as deposition continues. The resulting asymmetric peak is characteristic of multiple scattering phenomena associated with three-dimensional growth. The intensity of the Au ISS peak (Fig. 7) increases at a steady rate until 2 ML are deposited, at which point the slope abruptly decreases by a factor of 2, indicating that effectively one gold atom is hidden from the analysis beam for every two gold atoms deposited. This latter hypothesis will be studied by the method of angle-resolved ion scattering spectroscopy (ARISS) [14]. However, it should be

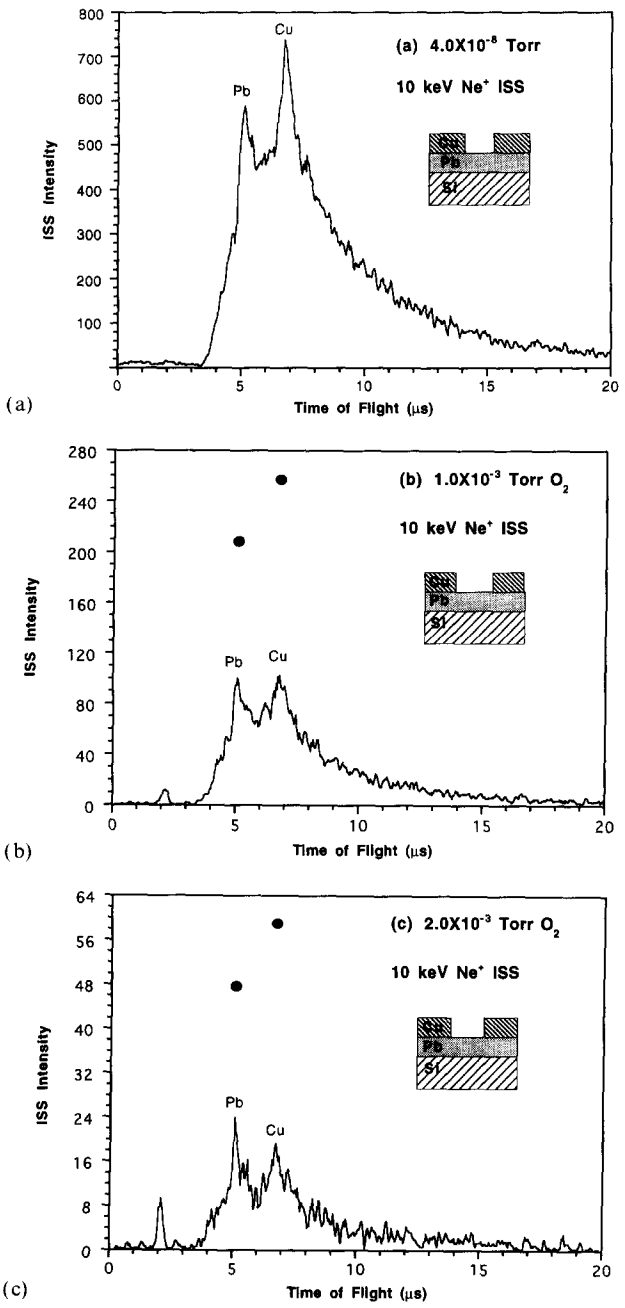


Fig. 8. 10 keV Ne^+ ion scattering spectra of CuPb ultrathin film in (a) an ultrahigh vacuum, (b) O_2 1×10^{-3} Torr and (c) O_2 at 2×10^{-3} Torr.

noted that this hypothesis is consistent with the formation of the ⟨100⟩ face of the f.c.c. gold lattice in that the second atomic layer is shifted by half a lattice spacing relative to the first layer, while the third layer is in registry with the first layer.

In order to demonstrate the effect of oxygen adsorption on the signal intensity, ~5.4 Å of Pb were deposited at room temperature onto a Si(100) substrate, followed by 4.4 Å of Cu. Fig. 8 shows the ISS data for a 10 keV Ne^+ beam incident on the sample at three different pressures of background O_2. The Cu peak exhibits a strong tail toward long flight times, and a large Pb signal is seen, even though approximately 2 ML of Cu was deposited on the Pb, indicating that the Cu "balled up" into three-dimensional islands, leaving exposed Pb.

As the oxygen pressure increases, the "prompt peak" at 2.1 μs, corresponding to primary ion-induced electron emission from oxidized surfaces increases in intensity [9]. At the same time, the intensity of the ISS peaks corresponding to Pb and Cu decrease. The data in Fig. 3(b) were used to calculate the anticipated decrease in intensity due to gas-phase scattering for Figs. 8(b) and 8(c) relative to Fig. 8(a). The calculated values are indicated in Figs. 8(b) and 8(c) by the full circles above the Pb and Cu peaks. Both the Pb and the Cu peak intensities are below the gas-phase scattering values. However, the Pb peak has stabilized at 50% of the gas-phase scattering value at a pressure of 1×10^{-3} Torr, indicating that a stable adsorbed oxygen layer or oxide has formed on Pb, while the Cu peak intensity continues to decrease, reaching a value of 32% of the scattering value at 2×10^{-3} Torr.

After pumping the chamber back to vacuum, the ion scattering spectrum changed completely back to the original situation (Fig. 8(a)). Therefore we conclude that oxygen chemisorption rather than oxide formation occurred, with preferential adsorption occurring on Cu.

5. Summary

We have developed a differentially pumped pulsed ion beam surface analysis system for in-situ real-time characterization of thin film growth processes in the presence of a relatively high pressure of ambient gas. The relationship between ISS and DRS signal intensities vs. the ambient pressure has been measured. Spectra with a reasonable signal-to-noise ratio have been obtained at ambient pressures up to 7 mTorr atmosphere in 2 min for the existing system geometry. Planned system modifications are expected to increase the pressure limit by a factor of 2–4. The real-time ISS analysis of Au deposition reveals that Au grows on the Si(100) surface in a two-dimensional layer-by-layer mode for at least first two monolayers. For a layered structure of 2 ML of Cu on top of a thin Pb layer, the Cu forms three-dimensional islands, leaving exposed Pb. At room temperature, oxygen adsorbs preferentially on the Cu portion of the surface.

Acknowledgments

This work has been supported by the US Department of Energy, BES-Materials Sciences, under Contract W-

31-109-ENG-38, as part of a cooperative research and development agreement between Argonne National Laboratory and the Ionwerks Corporation, and the Advanced Research Programs Agency under Grant N00014-93-1-0591.

References

[1] W. E. Quinn, D. E. Aspnes, M. J. S. P. Brasil, M. A. A. Pudensi, S. A. Schwarz, M. C. Tamargo, S. Gregory and R. E. Nahory, *J. Vac. Sci. Technol. B, 10* (2) (1992) 759.

[2] J. W. Rabalais, *J. Vac. Sci. Technol. A, 9* (3) (1991) 1293.

[3] M. Katayama, E. Nomura, N. Kanekama, H. Soejima and M. Aono, *Nucl. Instrum. Methods B, 33* (1988) 857.

[4] H. K. Schmidt, J. A. Schultz and Z. Zheng, in R. E. Clausing (ed.), *Diamond and Diamond-like Coatings*, Plenum, New York, 1991, p. 669.

[5] A. R. Krauss, M. Rangaswamy, Y. Lin, D. M. Gruen, J. A. Schultz, H. K. Schmidt and R. P. H. Chang, in O. Auciello and J. Engemann (eds), *Multicomponent and Multilayered Thin Films for Advanced Microtechnologies: Techniques, Fundamentals and Devices*, Kluwer, 1993, pp. 251–281.

[6] Y. L. Gavriljuk, V. G. Lifshits and N. Enebish, *Surf. Sci., 297* (1993) 345.

[7] Y. Tanishiro, M. Fukuyama and K. Yagi, *Materials Research Society Symp. Proc.*, Vol. 280, Materials Research Society, Pittsburgh, PA, 1993, p. 109.

[8] I. Hashim, B. Park and H. A. Atwater, *Materials Research Society Symp. Proc.*, Vol. 280, Materials Research Society, Pittsburgh, PA, 1993, p. 327.

[9] A. R. Krauss, Y. Lin, O. Auciello, G. J. Lamich, D. M. Gruen, J. A. Schultz, K. Waters and R. P. H. Chang, *J. Vac. Sci. Technol. A, 12* (4) (1994) 1943.

[10] J. F. Mahoney, J. Perel and A. T. Forrester, *Appl. Phys. Lett., 38* (5) (1981) 320.

[11] A. R. Krauss, O. Auciello, A. I. Kingon, M. S. Ameen, Y. L. Liu, T. Bar, T. M. Graettinger, S. H. Rou, C. S. Soble and D. M. Gruen, *Appl. Surf. Sci., 46* (1990) 67.

[12] A. I. Kingon, O. Auciello, M. S. Ameen, C. S. Soble, T. M. Graettinger, S. H. Rou and A. R. Krauss, in B. V. Hiremath (ed.), *Proc. Symp. on Thin and Thick Films, Acers, Westerville, OH, 1991*, Columbus, OH, 1991, American Ceramic Society, Columbus, OH, 1991, p. 147.

[13] A. V. Phelps, *J. Phys. Chem. Ref. Data., 20* (1991) 557.

[14] Y. Lin, A. R. Krauss, O. Auciello, Y. Nishino, D. M. Gruen, R. P. H. Chang and J. A. Schultz, *J. Vac. Sci. Technol. A, 12* (4) (1994) 1557.